Journal of Statistical Physics, Vol. 75, Nos. 5/6, 1994

Ising Model in an External Field on a Hierarchical Lattice

F. T. Lee[1] and M. C. Huang[1]

Received November 16, 1993; final February 21, 1994

The two-dimensional renormalization map of the diamond-hierarchical Ising model in an external field is given, and pictures of the distribution of zeros of the partition function in the complex plane of temperature for varying values of coupling constant and external field are shown. Critical exponents of the model are found, and results are different from those of the Ising model on a two- or three-dimensional regular lattice.

KEY WORDS: Zero; partition function; renormalization map; fixed point; critical exponents.

1. INTRODUCTION

Recently, hierarchical spin models[1-5] have received much attention in the literature owing to some particular properties of the models. First, hierarchical lattices[6] are constructed by decorating each bond with some basic cell iteratively such that the renormalization approximation of Migdal[7] and Kadanoff[8] becomes exact. In other words, in the context of the Migdal–Kadanoff renormalization, a variety of hierarchical spin models become exactly solvable. Second, a remarkable richness of phenomena has been revealed from these solutions. In general the partition function has an infinite number of zeros in the complex plane of temperature, which is essentially the Julia set of a rational map.[9,10] The Julia set exhibits multifractal structure,[11-13] and the free energy near the ferromagnetic transition point exhibits spatially modulated structure.[9,10] In some models with frustration the renormalization map may have chaotic trajectories which are suggested to correspond to a spin-glass phase.[14] From another aspect, because these hierarchical models are highly inhomogeneous in the coor-

[1] Department of Physics, Chung Yuan Christian University, Chung-Li, Taiwan. CYCUT∅37@twnmoe10.bitnet.

0022-4715/94/0600-1119$07.00/0

dination number of lattice sites and lack of translational invariance, one may expect these models to deepen our understanding of physical systems such as random magnets, polymers, and percolation clusters.[1,15,16]

To have a complete understanding of hierarchical spin models, an external field has to be added to the models. However, because of the inhomogeneity in the coordination number of lattice sites, the exact treatment of external fields on hierarchical spin models is very complicated. The exact renormalization map of the diamond-hierarchical Ising model in an external field was first given by McKay and Berker,[17] who divided magnetic fields into sites and bonds, and a site field always induces a bond field while itself remaining invariant under the renormalization map. In the present work, the diamond-hierarchical Ising model in an external field also is studied, but without introducing bond fields. The exact two-dimensional renormalization map is given first. Through the analysis of the given renormalization map, we then study how an external field affects the distribution and structure of the zeros. Finally, the thermodynamic properties of the model system are studied.

The paper is organized as follows. In Section 2, the diamond-hierarchical Ising model in external field is discussed, the two-dimensional renormalization map of the model is given, and the fixed points of the map are discussed. In Section 3, the distribution of zeros of the partition function and the effect of external field and coupling constant on the distribution of zeros are studied with the use of pictures. Thermodynamic quantities of the model and critical exponents near the ferromagnetic transition point are presented in Section 4.

2. THE MODEL AND ITS RENORMALIZATION MAP

Hierarchical lattices are constructed by infinite iteration procedures such that the Migdal–Kadanoff renormalization approximation can have exact realizations. Starting with a single bond, one can construct a larger and larger hierarchical lattice through a self-similar iterative procedure as follows. Each bond of the previous lattice is replaced by some basic cell in one iteration step, and after infinite iterations it results in a self-similar, inhomogeneous lattice with infinite number of lattice sites. The construction of the diamond-hierarchical lattice is schematized in Fig. 1,[18] where each bond is decorated by four bonds. The finite lattice constructed after n steps has site number $\frac{2}{3}(4^{n-1}+2)$ and bond number 4^{n-1}.

To define the Ising model on the diamond-hierarchical lattice, Ising spin is placed on each lattice site, and the Hamiltonian is

$$H = -J \sum_{\langle i,j \rangle} \delta(\sigma_i, \sigma_j) - h \sum_i \sigma_i \tag{1}$$

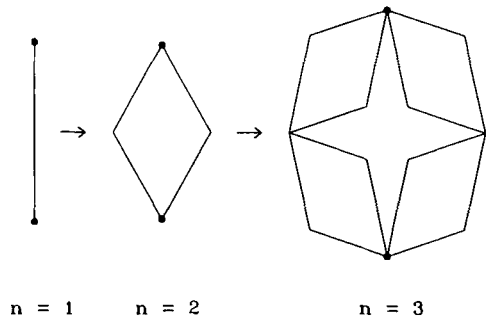

Fig. 1. The first two levels in the iterative construction of the diamond-hierarchical lattice.

where the first sum runs over all pairs of nearest neighbors, δ is the usual Kronecker delta function, the Ising spin σ_i has two possible values, $+1$ and -1, and the coupling constant J and external field h are two parameters. The partition function for the model on the finite lattice constructed after n steps is given by

$$Z_n = \sum_{\{\sigma\}} \exp\left[K_1 \sum_{\langle i,j \rangle} \delta(\sigma_i, \sigma_j) + K_2 \sum_i \sigma_i \right] \tag{2}$$

Here $K_1 = \beta J$, $K_2 = \beta h$, and $\beta = 1/kT$, with k the Boltzmann constant and T the temperature. For the model defined on the diamond-hierarchical lattice, all symmetries associated with the Hamiltonian remain the same as the model defined on a regular lattice. However, because the lattice is highly inhomogeneous, the translational invariance is completely lost.

To find the partition function with the renormalization map, let us review the well-known case where $K_2 = 0$ first.[9,10] To simplify notations, two variables, $y_1 = e^{K_1}$ and $y_2 = e^{K_2}$, are introduced. Without external field, i.e., $y_2 = 1$, the recursion relation between the partition functions for the model on the finite lattices constructed after n steps and $n-1$ steps is

$$Z_n(y_1) = Z_{n-1}(y_1')[A(y_1)]^{2 \times 4^{n-2}} \tag{3}$$

where the function $A(y_1)$ is given by

$$A(y_1) = 2y_1 \tag{4}$$

and y_1' is the image of y_1 under the renormalization map M defined as

$$y_1' = M(y_1) = \tfrac{1}{4}(y_1 + y_1^{-1})^2 \tag{5}$$

By the use of the recursion relation, Eq. (3), together with

$$Z_1(y_1) = 2(y_1 + 1) \tag{6}$$

one can obtained all of the information of the system defined by the model.

When an external field appears, the partition function at the first level, expressed in terms of two additional variables $a = y_1 y_2$ and $b = y_1 y_2^{-1}$, becomes

$$Z_1(a, b, y_2) = ay_2 + by_2^{-1} + 2 \tag{7}$$

The general recursion relation between the partition functions at the nth level and the $(n-1)$th level is found to be

$$Z_n(a, b, y_2) = Z_{n-1}(a', b', y_2)[B(a, b)]^{2 \times 4^{n-2}} \tag{8}$$

where the function $B(a, b)$ is defined as

$$B(a, b) = a + b \tag{9}$$

and a' and b' are the images of a and b under the two-dimensional renormalization maps M_1 and M_2 defined as

$$a' = M_1(a, b, y_2) = \left(\frac{a^2 + 1}{a + b}\right)^2 y_2^{-1} \tag{10}$$

and

$$b' = M_2(a, b, y_2) = \left(\frac{b^2 + 1}{a + b}\right)^2 y_2 \tag{11}$$

Note that y_2 in Eqs. (8),)10), and (11) remains the same as the initial value. The renormalization map found here is highly nonlinear, and the time-reversal symmetry, which is the symmetry associated with the Hamiltonian when the external field appears and corresponds to the interchange between y_2 and y_2^{-1}, is preserved in the map, and all results reduce to those of the case where an external field is absent by setting $y_2 = 1$.

The phase diagram of the model can be determined from the fixed points of the renormalization map, and one can study the property of a fixed point from the eigenvalues of the linearized map around the fixed point. For the two-dimensional map here, there are two eigenvalues Λ_{K_1} and Λ_{K_2} associated with the two directions K_1 and K_2 of the flow of the renormalization map. An attracting fixed point, for which both eigenvalues are less than 1, represents a thermodynamic phase. A saddle point has one eigenvalue larger than 1 and another less than 1, and a renormalization

map will drive the point to move along the direction of the eigenvalue larger than 1. The point with both eigenvalues larger than 1 is a repelling fixed point, and it represents a phase transition. The fixed points of the renormalization map, defined by Eqs. (10) and (11), can be obtained by solving the two coupled equations

$$a_f = M_1(a_f, b_f, y_2^f) \tag{12}$$

$$b_f = M_2(a_f, b_f, y_2^f) \tag{13}$$

where a_f and b_f are defined as $y_1^f y_2^f$ and y_1^f/y_2^f, respectively. The physical region of y_1 is $0 < y_1 < 1$ for the antiferromagnetic case and $1 < y_1 < \infty$ for the ferromagnetic case, while the region of y_2 is $0 < y_2 < \infty$. If y_1^f is set to be 1, Eqs. (12) and (13) reduce to an identity equation for y_2^f, and one has a set of solutions $\{y_1^f = 1 \text{ and } 0 < y_2^f < \infty\}$. The eigenvalues of the linearized map around any point belonging to the set are $\Lambda_{K_1} = 0$ and $\Lambda_{K_2} = 2$, and it implies that the flow of renormalization transformation goes ultimately to the sink $(y_1^s = 1,\ y_2^s = 0)$ for $0 < y_2^f < 1$, and to the sink $(y_1^s = 1,\ y_2^s = \infty)$ for $1 < y_2^f < \infty$. If one set $y_2^f = 1$, the possible values of y_1^f are 1, 3.38297..., and ∞. For $y_1^f = y_2^f = 1$, one has $\Lambda_{K_1} = 0$ and $\Lambda_{K_2} = 2$, and under the renormalization transformation this point moves ultimately to the sink $(y_1^s = 1,\ y_2^s = \infty)$ for the external field $h > 0$, and to the sink $(y_1^s = 1,\ y_2^s = 0)$ for $h < 0$. For $y_1^f = 3.38297...$, the eigenvalues of the linearized map are $\Lambda_{K_1} = 1.67857...$ and $\Lambda_{K_2} = 3.67857...$, and it corresponds to a repelling fixed point representing a ferromagnetic phase transition. The map also has two attracting fixed points at $y_1^f = \infty$ and y_1^f for $y_2^f = 1$ which are referred as the ferromagnetic and the paramagnetic fixed point, respectively. The qualitative behavior of the flow of the renormalization transformation obtained here is essentially the same as the Ising model on a two-dimensional regular lattice.[19]

3. THE ZEROS OF THE PARTITION FUNCTION

To see the distribution of zeros of the partition function in the complex plane of temperature, one notices that if zeros of the partition function for the finite lattice constructed after $n-1$ steps are known and denoted by $\tilde{a}_{n-1}(i)$ and $\tilde{b}_{n-1}(i)$ for the ith zero, then the zeros at the nth level, which are denoted by $\tilde{a}_n(k_i)$ and $\tilde{b}_n(k_i)$ for the kth zero associated with the ith zero at the $(n-1)$th level, can be found by solving the equations

$$\tilde{a}_{n-1}(i) = M_1(\tilde{a}_n(k_i), \tilde{b}_n(k_i), y_2) \tag{14}$$

$$\tilde{b}_{n-1}(i) = M_2(\tilde{a}_n(k_i), \tilde{b}_n(k_i), y_2) \tag{15}$$

This is the direct consequence of Eq. (8). Therefore, starting from the zeros of $z_1(a, b, y_2)$, in general one can find the limiting set of zeros of the partition function through backward iterations of the renormalization map step by step, and this limiting set forms an invariant set in a four-dimensional space spanned by complex y_1 and y_2.

For the case where external field is absent, Eqs. (14) and (15) reduce to a one-dimensional map,

$$\tilde{y}_{1,n-1}(i) = M(\tilde{y}_{1,n}(k_i)) \tag{16}$$

Sufficient backward iterations of the map with the initial value $y_1 = -1$, which is the zero of $Z_1(y_1)$, give the limiting set of the Yang–Lee zeros[20] of the partition function in the complex y_1 plane. The distribution of zero is simply the Julia set of the map.[9,10] There are two points here to be mentioned: the Julia set is an invariant set which is independent of the initial value of y_1, and instead of the backward iteration one can also use the forward iteration. If sufficient forward iterations are performed, various basins of attraction can be distinguished, and the boundary between different basins of attraction is made up of the unstable fixed points which belong to the set of zeros of the partition function. By the use of forward iterations, the resultant unstable fixed points are shown in Fig. 2a. In Fig. 2a, one can see clearly that in addition to the ferromagnetic transition located at $y_1 \approx 3.383$, there is an antiferromagnetic transition at $y_1 \approx 0.296$.

For the case where an external field appears, one has to specify the magnitude of external field h (coupling constant J) in terms of coupling constant J (external field h) in order to see the distribution of the zeros in the complex y_1 (y_2) plane. Because the real situation corresponds to the system in the thermodynamic limit, we therefore specify the magnitude when the system is defined on the infinite lattice. The specific magnitude changes according to Eqs. (10) and (11) when the renormalization map is performed. With the relation $h = \theta J$ or $J = \theta' h$, where θ and θ' are positive and real, specified on the infinite lattice, the set of the unstable fixed points is only a subset of the invariant set in a four-dimensional space, and one can only perform forward iterations to take account of the specified relation on the infinite lattice. When one performs sufficient forward iterations to obtain basins of attraction, then closures of the boundaries between different basins of attraction give the set of unstable fixed points which also is the set of the zeros in the complex y_1 or y_2 plane.

To see the distribution of zeros of the partition function in the complex y_1 plane, an external field h is specified by the relation $h = \theta J$ when the system is on the infinite lattice. According to the analysis of fixed points in Section 2, there are two basins of attraction; one belongs to the

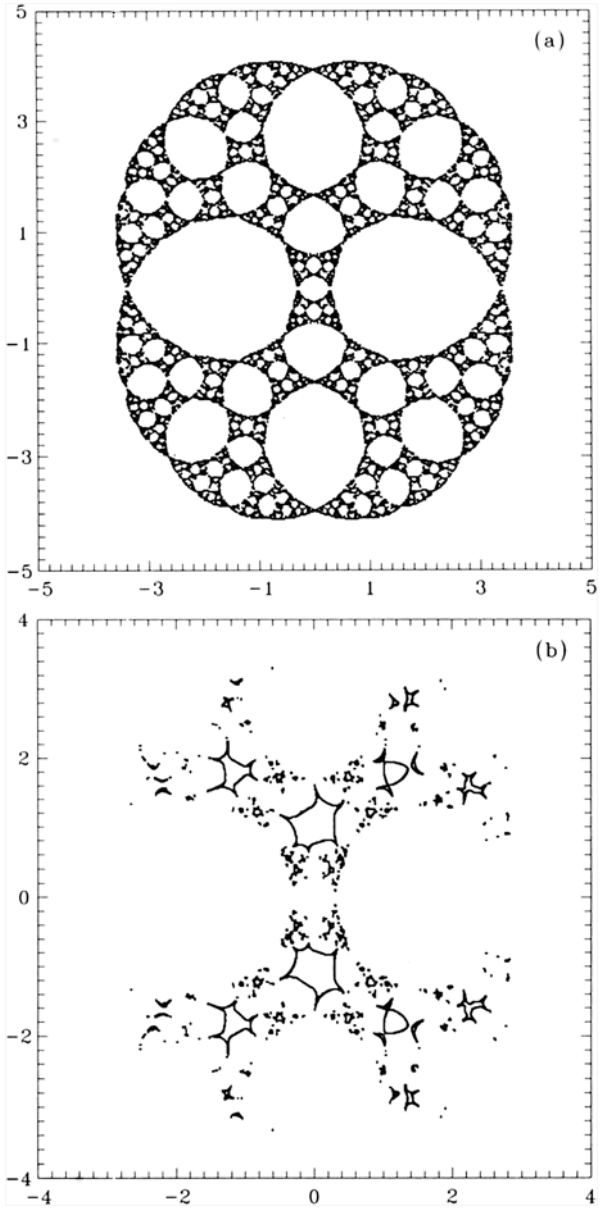

Fig. 2. The zeros of the partition function in the complex y_1 plane in the thermodynamic limit, obtained by forward iterations as explained in the text. The external field is specified by the relation $h = \theta J$ in the thermodynamic limit with (a) $\theta = 0$, (b) $\theta = 0.01$, (c) $\theta = 0.1$, (d) $\theta = 1$, (e) $\theta = 10$, and (f) $\theta = 100$.

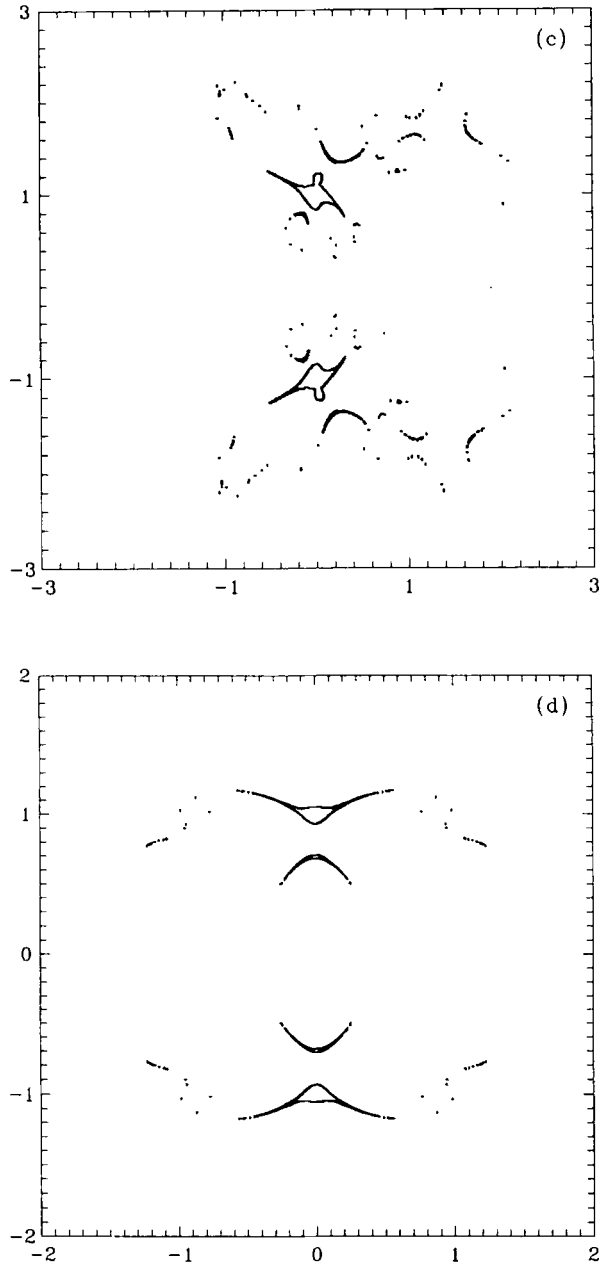

Fig. 2. (*Continued*)

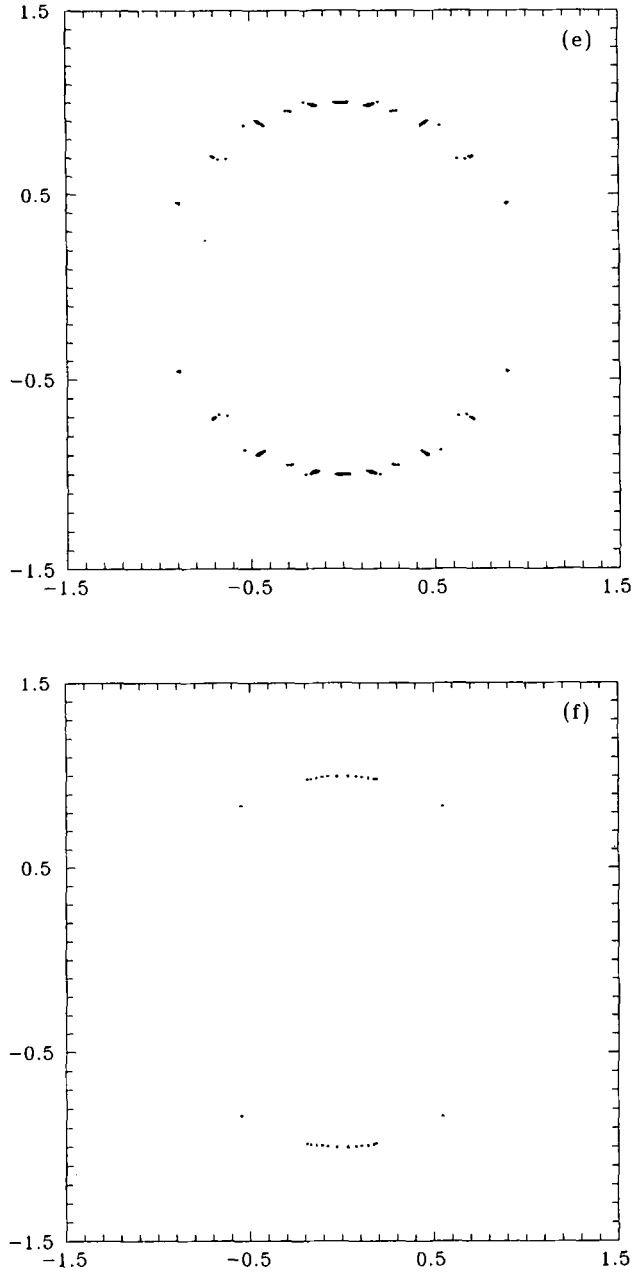

Fig. 2. (*Continued*)

ferromagnetic fixed point, $y_1^f = \infty$, and the other is the paramagnetic fixed point, $y_1^f = 1$. The closures of the boundaries between two different basins of attraction for different values of θ are shown in Figs. 2b–2f. From Figs. 2a–2f, one can see that the motion of the zeros caused by the external field is highly nonlinear, which is due to the nonlinearity of the renormalization map. Qualitatively, once a tiny external field appears, the zeros move away from the real axis, then approach a circle with increasing h, and finally disappear in the limit of $\theta \to \infty$. There is no zero falling on the real axis, and this implies that only one phase exists in the physical region for $h \neq 0$.

The process of obtaining the distribution of the zeros in the complex y_2 plane is the same as the one in the complex y_1 plane except that the coupling constant J is specified by the relation $J = \theta' h$. In the y_2 plane, there are also two kinds of basins of attraction, one for $y_2^s = \infty$ and the other for $y_2^s = 0$. When $\theta' = 0$, there are only two zeros, i and $-i$, for the partition function. The zeros become rich for nonvanishing θ' as shown in Figs. 3a–3e for varying θ' values. From Figs. 3a–3e, one can see that the distribution of the zeros almost falls on a unit circle with fractal structure when θ' is very large, and more fine resolution is needed to see the fractal

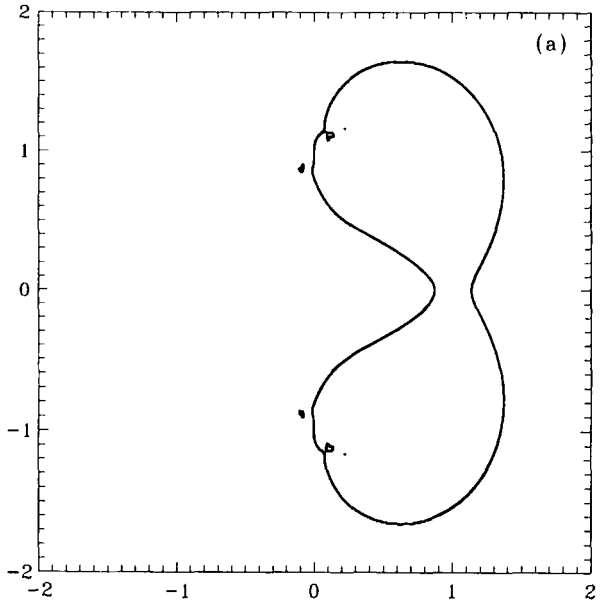

Fig. 3. The zeros of the partition function in the complex y_2 plane in the thermodynamic limit, obtained by forward iterations as explained in the text. The coupling constant is specified by the relation $J = \theta' h$ in the thermodynamic limit with (a) $\theta' = 0.01$, (b) $\theta' = 0.1$, (c) $\theta' = 1$, (d) $\theta' = 10$, and (e) $\theta' = 100$.

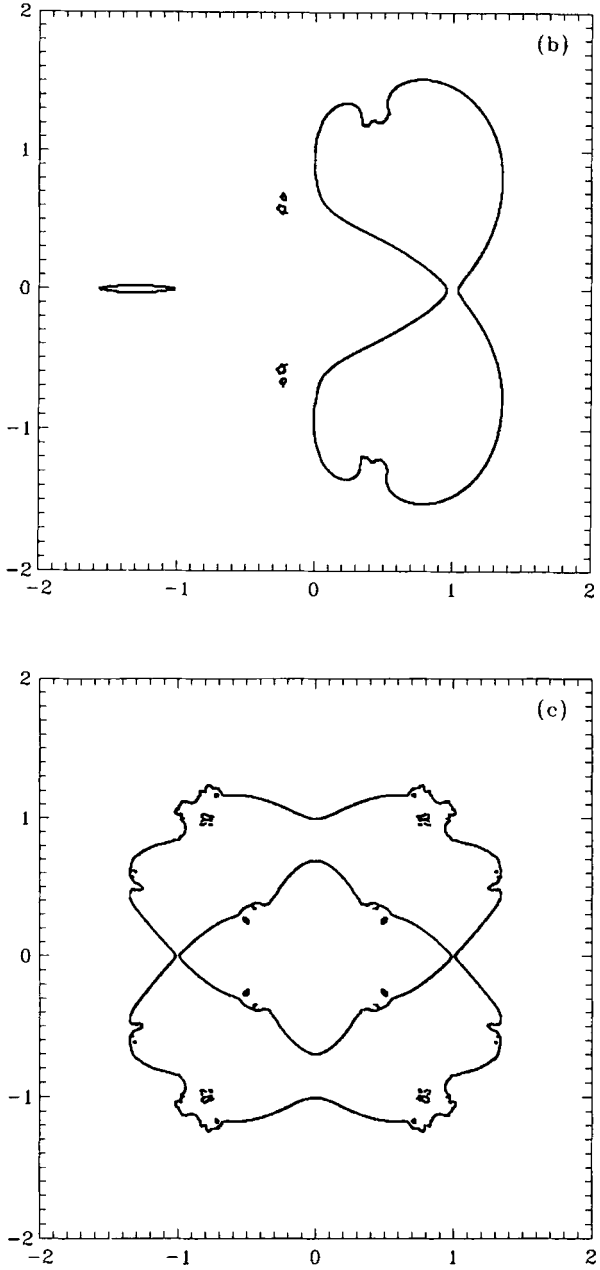

Fig. 3. (*Continued*)

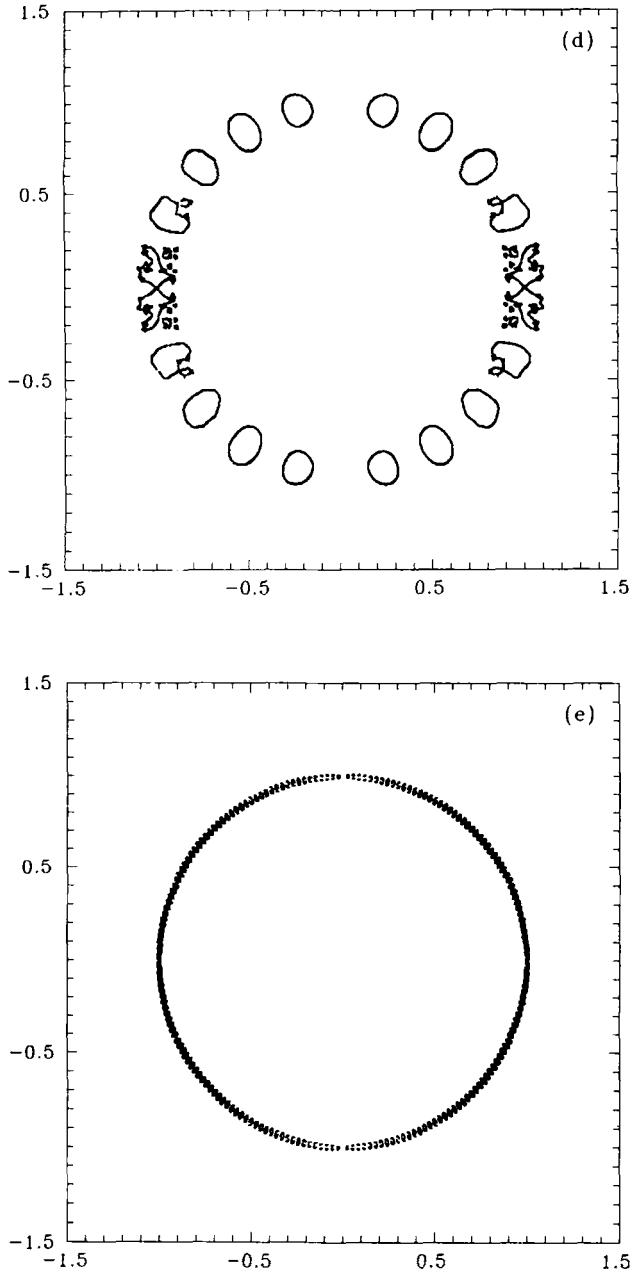

Fig. 3. (*Continued*)

structure for θ' approaching to the limit of $\theta' \to \infty$. We note that it appears in Figs. 3a and 3b that there are two zeros falling on the positive real axis; this is caused by the limitation of resolution. In fact there is only one point falling on the positive real axis for all values of θ', and this point is the saddle point of $y_2 = 1$.

In obtaining Figs. 2a–2f and 3a–3e, the distributional region of the zeros in the complex y_1 or y_2 plane is coarse-grained, and forward iterations of the renormalization map are performed up to 16 times at each point to determine the basin of atraction to which the point belongs. The resolution of each figure depends on the interval between the two nearest points, and the typical chosen interval is about 0.2, depending on how large the distributional region of the zeros is. Note that Fig. 2a is invariant in the change $y_1 \to 1/y_1$ or $y_1 \to -y_1$, due to the same symmetry maintained by the map, while the invariance is broken by the specified relation $h = \theta J$ or $J = \theta' h$ in other figures.

4. THERMODYNAMIC QUANTITIES AND CRITICAL EXPONENTS

Various thermodynamic quantities can be obtained by the derivatives of the free energy. The functional equation for the reduced free energy per bond can be obtained from the recursion relation, Eq. (8), obeyed by the partition function, and the result is

$$f[M_1(a, b, y_2), M_2(a, b, y_2), y_2] = 4f(a, b, y_2) + \frac{2}{\beta} \ln B(a, b) \qquad (17)$$

By the use of the above equation, one can obtain the following convergent representation of the free energy per bond:

$$f(a, b, y_2) = -\frac{1}{2\beta} \sum_{n \geq 0} \frac{1}{4^n} \ln B[M_1^n(a, b, y_2), M_2^n(a, b, y_2)] \qquad (18)$$

Note that the fixed point of the ferromagnetic phase transition is located at $y_1^f = 3.38297...$, which corresponds to the transition temperature at $kT_c/J = 0.82051...$. To find each thermodynamic quantity, the derivative of the free energy is replaced by the finite difference, and the summation in n of Eq. (15) is carried up to $n = 13$, in which the pseudocritical temperature at which the maximum of specific heat or susceptibility of a finite system occurs agrees with kT_c/J up to the fourth decimal place. The calculated thermodynamic quantities, which are expressed as dimensionless, are magnetization M, specific heat C/k, and susceptibility χJ, and the results are shown in Figs. 4a–4d, where the magnetization $M(T)$ and susceptibility

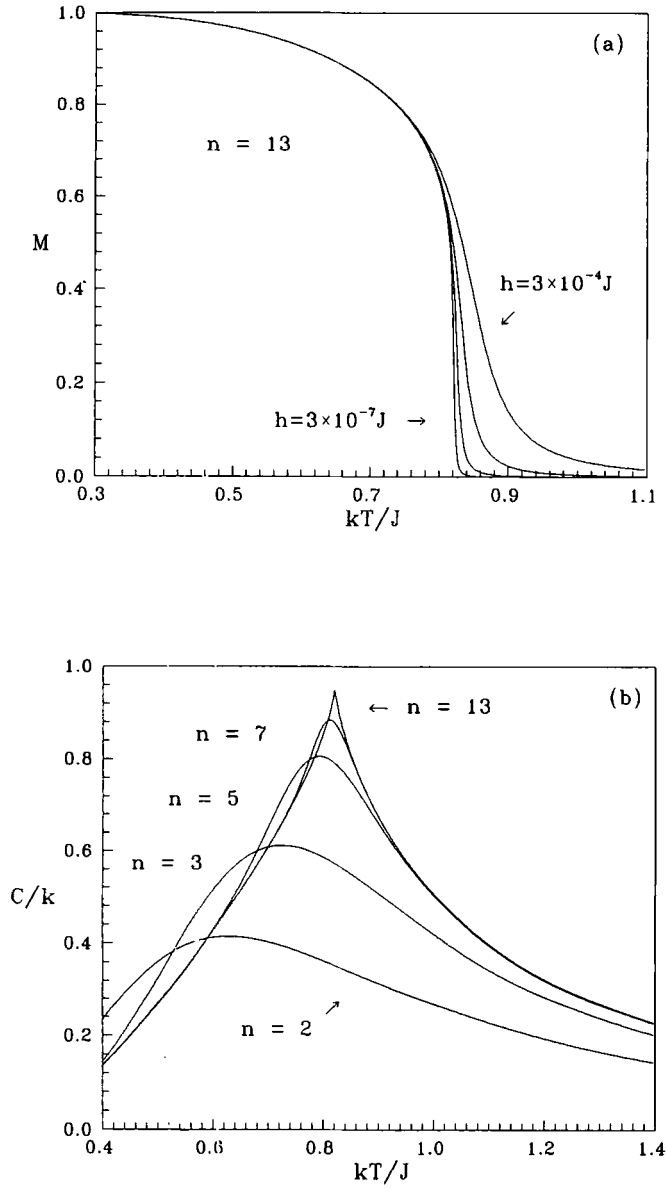

Fig. 4. Various thermodynamic quantities as a function of temperature: (a) $M(T)$; (b) $C(T)/k$; and (c) $\chi(T)J$ in units of 10^5. (d) The magnetization as a function of the external field.

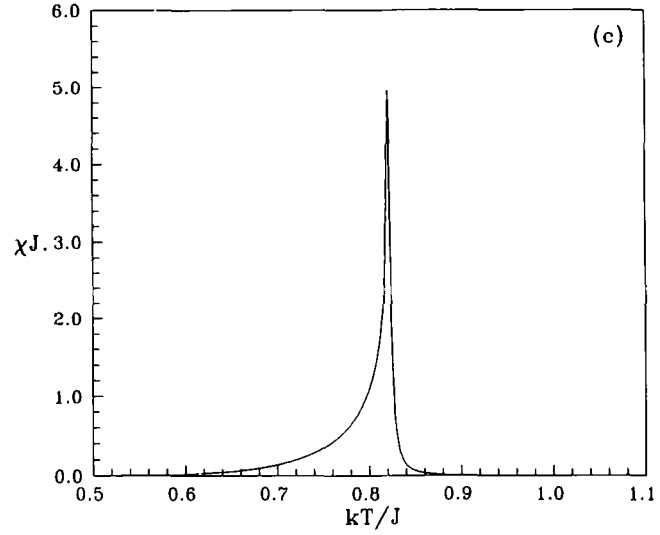

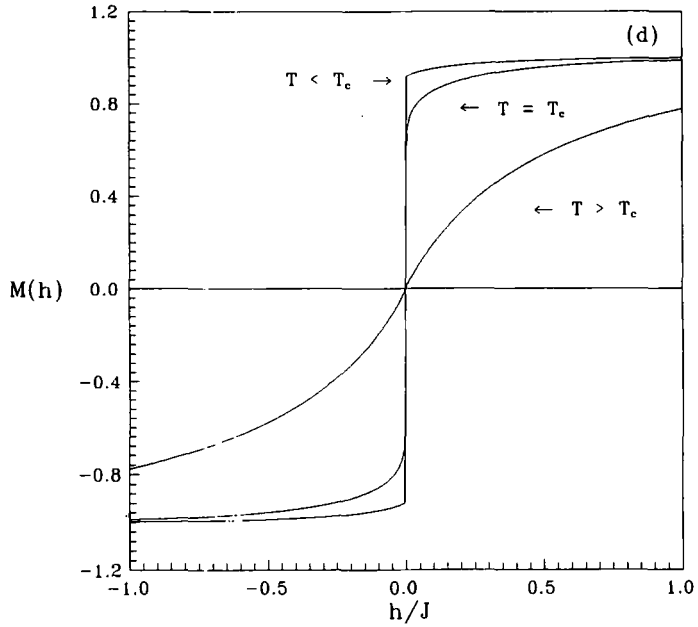

Fig. 4. (*Continued*)

Table I. Critical Exponents of the Ising Model on a Diamond-Hierarchical Lattice and on Two- and Three-Dimensional Regular Lattices

Type of lattice	α	β	γ	δ
Diamond-hierarchical	0.0150	0.1625	2.2625	15.3846
2D regular lattice	0	0.125	1.75	15
3D regular lattice	0.125	0.312	1.250	5.150

$\chi(T)J$ at $h=0$ are approximated by adding a tiny external field, $h=3\times10^{-7}J$, to the system to avoid the trouble caused by degenerate vacua for $T<T_c$.

For a second-order phase transition, the critical behavior near the phase transition point can be characterized by a set of critical exponents such as α, β, and γ defined by $C(T)\sim(T-T_c)^{-\alpha}$, $M(T)\sim(T_c-T)^{\beta}$, and $\chi(T)\sim(T-T_c)^{-\gamma}$ for temperature T near the critical temperature T_c of the infinite system. Another critical exponent δ, which is related to the behavior of magnetization at the critical point under the influence of the external field, is defined by $M(T_c)\sim|h|^{1/\delta}$ for a very small external field h. Critical exponents can be obtained by linearizing the renormalization map of Section 2 around the ferromagnetic transition point, but here we use the numerical method to obtain the result approximately. The exponents are extracted directly from the results of Figs. 4a–4d by finding the slopes from the logarithmic plots. Because of the spatially modulated structure of the free energy near the ferromagnetic transition point,[9,10] the range of temperature away from the critical temperature for the power law behavior of specific heat is much narrower compared with other quantities. The resultant critical exponents along with those for the model on two- and three-dimensional regular lattices are listed in Table I. The results shown in Table I indicate that the critical behavior of the diamond-hierarchical Ising model is different from that of the model defined on a two- or three-dimensional regular lattice.

5. CONCLUSION

In this paper, the two-dimensional renormalization map of the diamond-hierarchical Ising model an external field is given, and the information revealed from the map is studied. The unstable fixed points of the renormalization map give the zeros of the partition function, and the distribution of zeros in the complex plane of temperature is exhibited by the figures. It is believed that hierarchical spin models can have phase transition and nonclassical criticality at finite temperatures.[1,4] The critical

exponents of the diamond-hierarchical Ising model near the ferromagnetic transition point are obtained approximately by the numerical method, and the results exhibit nonclassical criticality clearly.

The invariant set of the renormalization map is defined on a four-dimensional space of the complex y_1 and y_2. It is interesting to know the general property of the four-dimensional invariant set, which is not touched by this paper. One has to keep in mind that hierarchical lattices are examples of fractal lattices. Features found on one fractal latice may not pertain for other fractal lattices or persist on regular lattices. In fact, it has been suggested[21] that a characterization of fractal lattices involves several factors: the fractal dimensionality, the topological dimensionality, the order of ramification , the connectivity, the lacunarity, etc. Then it is important to know how these factors are related to the unusual features appearing on hierarchical lattices, and some progress has been made along this direction.[17,18,21-23]

REFERENCES

1. A. N. Berker and S. Ostlund, *J. Phys. C* **12**:4961 (1979).
2. R. B. Griffiths and M. Kaufman, *Phys. Rev. B* **26**:5022 (1982).
3. N. M. Svrakic, J. Kertesz, and W. Selke, *J. Phys. A* **15**:L427 (1982).
4. B. Derrida, J. P. Eckmann, and A. Erzan, *J. Phys. A* **16**:893 (1983).
5. A. Erzan, *Phys. Lett. A* **93A**:237 (1983).
6. M. Kaufman and R. B. Griffiths, *Phys. Rev. B* **24**:496 (1981).
7. A. A. Migdal, *Sov. Phys. JETP* **42**:743 (1976).
8. L. P. Kadanoff, *Ann. Phys.* (N.Y.) **100**:359 (1976).
9. B. Derrida, L. De Seze, and C. Itzykson, *J. Stat. Phys.* **33**:559 (1983).
10. B. Derrida, C. Itzykson, and J. M. Luck, *Commun. Math. Phys.* **94**:115 (1984).
11. M. H. Jensen, L. P. Kadanoff, and I. Procaccia, *Phys. Rev. A* **36**:1409 (1987).
12. B. Hu and B. Lin, *Phys. Rev. A* **39**:4789 (1989).
13. B. Hu and B. Lin, *Physica. A* **177**:38 (1991).
14. S. McKay, A. N. Berker, and S. Kirkpatrick, *Phys. Rev. Lett.* **48**:767 (1982).
15. P. J. Reynolds, H. E. Stanley, and W. Klein, *Phys. Rev. B* **21**:1223 (1980).
16. M. S. Cao, *J. Stat. Phys.* **71**:51 (1993).
17. S. R. McKay and A. N. Berker, *Phys. Rev. B* **29**:1315 (1984).
18. M. Kaufman and R. B. Griffiths, *J. Phys. A* **15**:L239 (1982).
19. Th. Niemeijer and J. M. J. van Leeuwen, in *Phase Transitions and Critical Phenomena*, Vol. 6, C. Domb and M. S. Green, eds. (Academic Press, New York, 1976), p. 425.
20. C. N. Yang and T. D. Lee, *Phys. Rev.* **87**:404 (1952); T. D. Lee and C. N. Yang, *Phys. Rev.* **87**:410 (1952).
21. Y. Gefen, B. Mandelbrot, and A. A. Aharony, *Phys. Rev. Lett.* **45**:855 (1980).
22. J. R. Melrose, *J. Phys. A* **16**:1041 (1983).
23. J. R. Melrose, *J. Phys. A* **16**:3077 (1983).